Comparison of ultrafast intense-field photodynamics in aniline and nitrobenzene: stability under amino and nitro substitution

Journal:	*Physical Chemistry Chemical Physics*
Manuscript ID	CP-ART-12-2018-007866.R1
Article Type:	Paper
Date Submitted by the Author:	17-Feb-2019
Complete List of Authors:	Scarborough, Timothy; Ohio State University, Physics McAcy, Collin; University of Nebraska - Lincoln, Physics and Astronomy Beck, Joshua; University of Nebraska - Lincoln, Physics and Astronomy Uiterwaal, Cornelis; University of Nebraska - Lincoln, Physics and Astronomy

PCCP

ROYAL SOCIETY OF CHEMISTRY

ARTICLE TYPE

Cite this: DOI: 10.1039/xxxxxxxxxx

Comparison of ultrafast intense-field photodynamics in aniline and nitrobenzene: stability under amino and nitro substitution

Timothy D. Scarborough,[a] Collin J. McAcy,[b] Joshua Beck,[b] and Cornelis J. G. J. Uiterwaal[b]

Received Date
Accepted Date

DOI: 10.1039/xxxxxxxxxx

www.rsc.org/journalname

We report on the photoionization and photofragmentation of aniline ($C_6H_5NH_2$) and nitrobenzene ($C_6H_5NO_2$) under single-molecule conditions in the focus of 50-fs, 800-nm laser pulses. Ion mass spectra are recorded as a function of intensity ranging from 6×10^{12} to 3×10^{14} W/cm^2. Ion yields are measured in the absence of the focal volume effect and without the need for additional deconvolution of data. We observe evidence of resonance-enhanced multiphoton ionization in aniline, in agreement with current literature. Phenyl-based ion fragments, singly-charged parent ions, and dissociative rearrangement processes are observed for both molecules. However, fragmentation in aniline is heavily suppressed in favor of parent ionization while the reverse is true for nitrobenzene, and multiply-charged parent ions are present in aniline and absent in nitrobenzene. We discuss the implications of these and other results as they relate to molecular stability against intense-field ionization and fragmentation, specifically with regards to the opposing behavior of the substituted amino and nitro functional groups.

1 Introduction

The role of structural substitutions in molecules, and their ability to have profound effects on a molecule's ability to affect steady-state properties, has been explored for many decades. Only in recent years have the effects of such substitutions begun to be observed on ultrafast time scales. Atomic substitutions have been observed to frustrate high harmonic generation,[1] and nuclear vibrational dynamics sensitive to substitutions have been measured using electron diffraction.[2,3] As the field of ultrafast science has developed, larger systems of biological and chemical relevance have been studied,[4,5] and the electronic dynamics of ionization,[6,7] charge migration,[8–10] and conical intersections[3,11,12] have been explored, with substitutions affecting both nuclear and electronic behavior. With the increasing capability to measure such behaviors, the study of systematic atomic substitutions in organic and bio-relevant molecules and their responses to intense fields becomes increasingly important.

We choose to explore the benzene (C_6H_6) system and the effects substitutions have on the intense-field ionization to the system and its fragments. One type of substitution involves the removal of a hydrogen atom, and its replacement with a functional side-group. Previously we have investigated a variety of similar substitutions both within[13] and outside the ring;[14] here we investigate amino (NH_2) and nitro (NO_2) substitutions as side-groups. The molecules which result from this substitution, aniline and nitrobenzene, are structurally very similar, both comprised of a phenyl ring (C_6H_5, abbreviated 'Ph') with a single three-atom nitrogen-based functional group; these molecules are diagrammed in Fig. 1. However, the two substituted groups have opposite effects on the electron density of the phenyl ring: the amino group is highly electron-donating, pushing electron density from the group into the ring, and the nitro group is highly electron-withdrawing, pulling electron density out of the ring and into the group.[15] These differences contribute to the drastically different ionization potentials (IPs) of the two molecules—7.72 eV in aniline, compared to 9.94 eV in nitrobenzene,[16] differing C-N bond lengths,[17] and vastly different electron densities in both the σ and π structures[18] in steady-state calculations. However, direct experimental comparison of the way they affect intense-field photodynamics, especially with regards to the stability of aromatic molecules against ionization and fragmentation, has not been extensively studied. Further, due to the inherent complexity and computational cost of *ab initio* methods like time-dependent density functional theory or solutions of the time-dependent Schrödinger equation, calculations of the full dynamics of large molecules are scarce. Cataloguing the photodynamical differences resulting from the substitution of a single structural

[a] *Physics Research Building, Department of Physics, The Ohio State University, Columbus, Ohio 43210, USA. E-mail: scarborough.39@osu.edu*
[b] *Theodore Jorgensen Hall, Department of Physics and Astronomy, University of Nebraska-Lincoln, Lincoln, Nebraska 68588, USA.*

parameter is then doubly useful, as the information gained could potentially create new metrics against which quantum-chemical calculations could be compared.

To this end, we present a comparison of ion yields in aniline and nitrobenzene resulting from ultrafast, intense fields. Our data suggests that while the electron-donating nature of the amino group stabilizes aniline, suppressing photofragmentation and enhancing multiple photoionization, the electron-withdrawing nature of the nitro group destabilizes nitrobenzene with the opposite effects.

2 Experiment

We used 800-nm ($\hbar\omega = 1.55$ eV), 50-fs laser pulses generated by a Ti:sapphire laser system based on chirped pulse amplification and focused into a vacuum chamber using a plano-convex fused silica lens. The intensity of the beam is adjustable by means of a half-wave plate in the amplifier's compressor. Focal intensity values were calculated based on recorded pulse energies of up to 2.1 mJ and a measured beam waist of 38 μm. While the maximum intensity of our beam is on the order of 10^{15} W/cm^2, focal intensities in this particular experiment ranged from 6×10^{12} W/cm^2 to 3×10^{14} W/cm^2. At each intensity a time-of-flight (TOF) ion spectrum is recorded; Fig. 2 shows examples of spectra for aniline and nitrobenzene. Artifacts and inhomogeneity from nonlinear optical effects are expected to be negligible as the maximum B-integral[19] possible for our experimental conditions is on the order of unity.

Target molecules were introduced as vapor into an ultra-high vacuum chamber. The target vapor was held at a fixed pressure of 5×10^{-7} mbar, a value chosen to maximize the ion detection rate while minimizing pressure-related experimental artifacts. To avoid intensity gradients and minimize the effects of potential focusing aberrations, we collected ions in a sampling volume 1 mm away from the central focus on the defocusing side of the beam waist. We measured their TOF with a double microchannel plate, which interfaced with a counting card controlled by a computer.

Our reflectron-type TOF spectrometer maps spatial ion densities to a TOF spectrum in such a way that different portions of the ion peaks correspond to different regions in the sampling volume.[20] When calculating ion yields we chose a specific 15 μm $\times$ 15 μm $\times$ 500 μm region of the sampling volume over which the intensity was approximately constant (varying by less than 1/14$^{\text{th}}$ of a decade[14]) and only counted ions created within this region. All ions outside this region of interest were ignored. This method eliminates focal averaging and allows us to view molecular processes that would otherwise be obscured, such as resonance-enhanced multiphoton ionization (REMPI).[20] TOF values are converted to mass-per-charge (m/q) values using simple kinematics;[20,21] ion mass spectrum data are then displayed as a function of m/q values, as this allows for easy identification of ion species corresponding to observed peaks. Samples of aniline and nitrobenzene, of $\geq 99.5\%$ and $\geq 99.0\%$ purity respectively, were procured from Sigma-Aldrich and used as purchased.

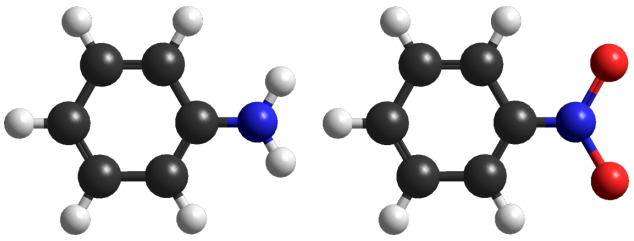

Fig. 1 Molecular models of aniline (left) and nitrobenzene (right). Note that the only structural difference between the two molecules is the substituted functional groups: an amino group –NH_2 in aniline, and a nitro group –NO_2 in nitrobenzene.

3 Results

3.1 Parent ionization

Shown in Fig. 3 are the intensity-dependent yields of parent ions for aniline. At all intensities studied, the most abundant ion found in the aniline mass spectra is the singly-ionized parent molecule ($m/q = 93$), followed by the doubly-ionized parent molecule ($m/q = 46.5$) and $C_5H_5^+$. Triply-ionized aniline ($m/q = 31$) is uncommon (see Fig. 3), but non-negligible at intensities above 10^{14} W/cm^2. The aniline parent ion yield has two regions of approximately integer log-log slope, illustrated in Fig. 3: a low-intensity region with of slope 5.00 ± 0.06, and a higher-intensity region of slope 3.02 ± 0.06. Data points included in each fit satisfy three criteria. First, points are included sequentially by intensity without skipping, so that all points in a given intensity range contribute to the slope fit. Second, excluding points from the range should have a negligible effect on the slope value and residuals; this ensures that the lowest- or highest-intensity points in the range are not adversely altering the slope. Finally, including additional points results in either a drastically different slope value or a much higher sum of residuals. If either the slope or the residuals are affected, the intensity is outside of the region accurately defined by the I^n power law of multiphoton ionization,[22,23] (in which I is the field intensity and n the photon number) and the points are excluded from the fit.

It should be noted that the power law fits are only valid for a leading-order process, and thus cannot be used to extract quantitative information about the ionization process which results in the doubly- or triply charged parent ions, or from fragmentation channels. Fragmentation, in particular, can be induced either during or following ionization, or as the result of multiply-charged ions decaying into a collection of singly-charged fragments. The complexities of these processes are not revealed by ion mass spectrometry alone, and therefore speculation over the precise mechanisms will not be employed in the present work.

In contrast to aniline, parent ionization in nitrobenzene ($m/q = 123$) is heavily suppressed (see Fig. 2), especially when compared to prominent fragments (see Fig. 4); at none of the measured intensities is the parent ion within a factor of 10 of the leading-order ionic fragment. Doubly-charged nitrobenzene parent ions ($m/q = 61.5$) are entirely absent from recorded ionization spectra. Note also that the nitrobenzene parent ion yield saturates at a much lower intensity ($\sim 6\times10^{13}$ W/cm^2) than the aniline parent ion yield ($\sim 2.5\times10^{14}$ W/cm^2); this does not represent saturation of the ionization rate, but is instead due to the near-

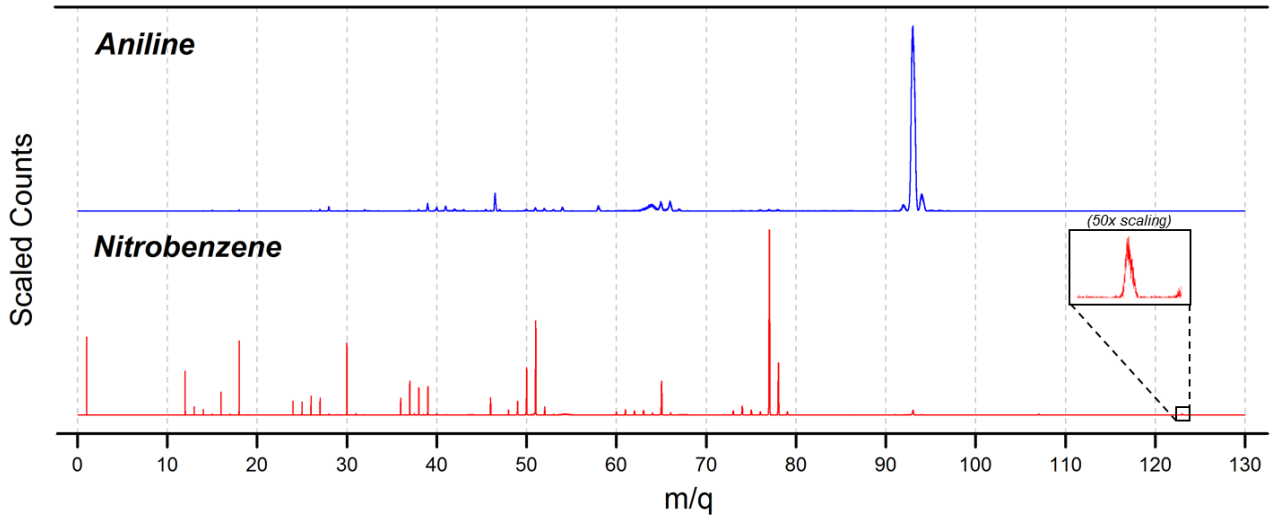

Fig. 2 Ion mass spectra of aniline and nitrobenzene for qualitative comparison, recorded at a focal intensity of 10^{14} W/cm^2 and scaled to emphasize relative yields of various ions. The nitrobenzene parent peak has been enhanced for visibility.

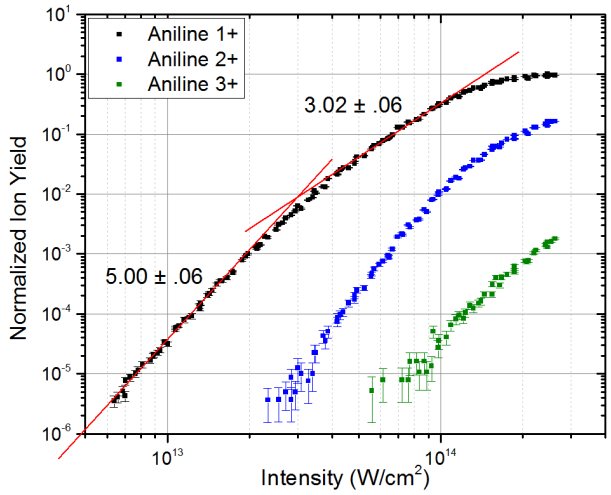

Fig. 3 Yields of multiply-charged aniline ions, plotted as a function of intensity in a double-logarithmic representation. The singly-charged ion curve has two regions of approximately integer slope; red lines drawn through these regions represent exact integer slopes and are meant to guide the eye. Error-weighted, fit-calculated slope values for each region are shown next to their respective regions. Data points included in each fit satisfy three criteria: (1) points are included sequentially by intensity without skipping; (2) excluding points has negligible effects on slope value and residuals; and (3) including additional points results in either a drastically different slope value or a much higher sum of residuals.

complete molecular fragmentation affecting the rate at which singly-charged ions are measured.

3.2 Fragmentation

Both aniline and nitrobenzene have rich ion spectra with numerous features of interest. Fig. 4 highlights a few key differences in the dissociation dynamics of the two molecules by showing ion yields of some fragments found in both molecules' ion spectra. At a glance, the most striking difference is the abundance of fragment ions in relation to the parent ions: fragmentation in aniline is suppressed in favor of parent ionization, and the reverse is true for nitrobenzene. It should be noted that yields of NH_2^+ should not be taken as quantitatively meaningful; their m/q ratio overlaps with smaller ions such as CH_4^+, O^+, and doubly ionized O_2. They are presented here to display the comparative scarcity relative to other fragments, but can be viewed only as an upper limit to a NH_2^+ yield.

However, to discuss more specific differences between the two molecules, it becomes useful to sort observed fragments into groups. The first group of interest includes fragments made entirely of carbon and hydrogen atoms, which can be further categorized by the number of carbon atoms in the ionic fragment. Aniline most commonly dissociates into fragments leaving ions in the C_5 group (those with 5 carbon atoms), followed by those in the C_3, C_4, and C_6 groups respectively. Nitrobenzene follows a reverse pattern, tending to dissociate into C_6-group ions followed by those in the C_4, C_3, and C_5 groups respectively. Phenyl ions are the most abundant ions in all recorded nitrobenzene spectra but are quantitatively unremarkable in the aniline spectra.

A second group of interest, yields of which are shown in Fig. 5, includes $PhNX_2^+$ (the parent), $PhNX^+$, PhN^+, PhX^+, and Ph^+, where X is a placeholder for either O or H. This group includes fragments with an empirically intact phenyl ring, fragments with

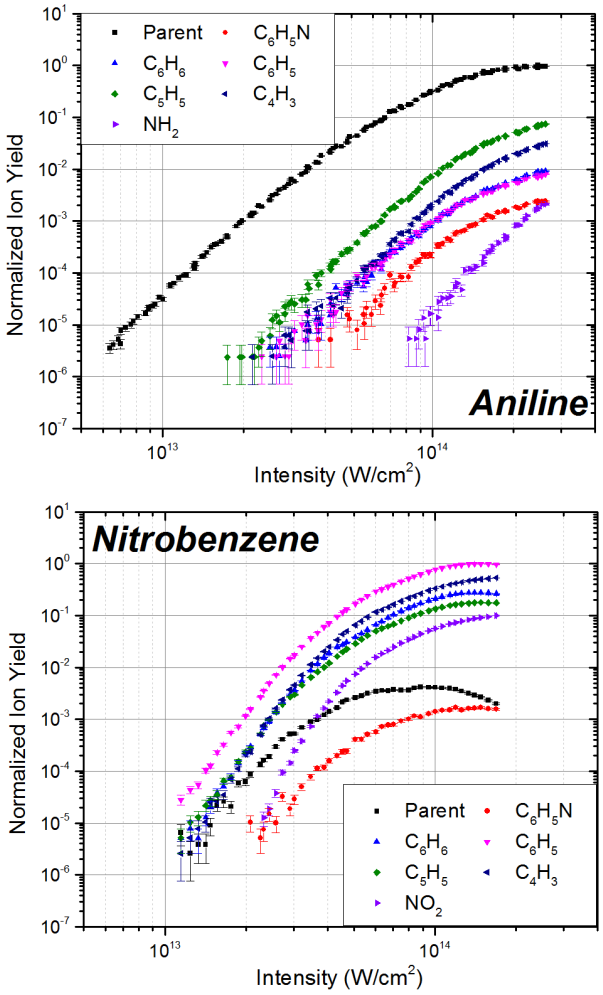

Fig. 4 Yields of some ions common to both aniline and nitrobenzene, plotted as a function of intensity in a double-logarithmic representation. Ion counts have been normalized such that the highest recorded fragment yield (the parent ion in aniline, and the $C_6H_5^+$ fragment in nitrobenzene) is set to unity; all other fragments are thus represented as a relative ratio to the maximum.

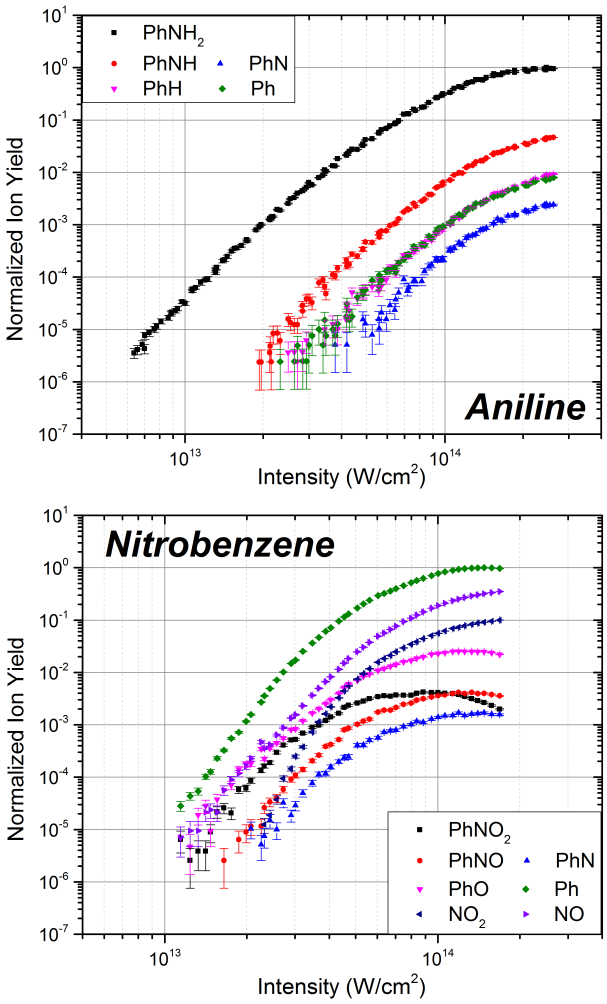

Fig. 5 Yields of ions related to the dissociative decay of the amino and nitro functional groups, plotted as functions of intensity and displayed in double-logarithmic representations. Ion counts have been normalized as in Fig. 4, making the highest recorded yield of any single ion exactly 1 for each target molecule.

either partial or complete loss of their respective functional group, and the parent ions for comparison. Over all recorded intensities, the yield of aniline's parent is anywhere from one to four orders of magnitude greater than the yields of any other ion in this group, likely indicating that aniline is more likely to undergo parent ionization than to lose atoms from its amino group. For nitrobenzene, PhN^+ and $PhNO^+$ ($m/q = 107$) are the rarest ions in this group. The third ion group includes NX_2^+ and NX^+, where X is again a placeholder for either O or H. These fragments are expected to be correlated to the functional group decay discussed above. For example, in the nitrobenzene spectra, phenyl ions are the most abundant fragments observed, suggesting that the nitro group as a whole is prone to dissociation from the phenyl ring. However, NO^+ ($m/q = 30$) is more abundant than NO_2^+ ($m/q = 46$), indicating that the nitro group is itself prone to breaking apart following a dissociation. On the other hand, phenyl yields in aniline are heavily suppressed. When paired with the robust presence of $PhNH^+$ ($m/q = 92$), the suppression sug-

gests that aniline tends to lose its amino group piecewise or not at all, depending on if the missing hydrogen atoms generally originate from the amino group or the ring (again, isomers are indistinguishable in our data). It should be mentioned that ions in this group related to aniline are absent from Fig. 5; as metioned above, NH_2^+ ($m/q = 16$) and NH^+ ($m/q = 15$) have the same m/q value as other possible ions, preventing their analysis in a quantitative manner.

4 Discussion

4.1 Multiphoton ionization

In a multiphoton ionizaton (MPI) process, the probability of an n-photon ionization is proportional to I^n at low intensities.[22,23] Such a process would then present itself as an integer slope in a double-logarithmic representation of ionization yield plotted against intensity. The ionization potential of aniline is 7.72 eV, just within reach of the combined energies of five 800-nm photons. MPI in aniline would then occur from the molecule's highest-occupied molecular orbital (HOMO) and show a low-intensity log-log slope of 5, which we observe (see Fig. 3). We also observe a log-log slope of 3 at higher, pre-saturation intensities. Given that 3-photon excitations near 800 nm have been previously observed in neutral aniline,[24–26] the lifetimes of these resonant states are longer than our 50-fs pulse duration,[24] and observed fragmentation is negligible compared to yields of singly-ionized aniline (see Fig. 4), it is likely that aniline undergoes (3+2) REMPI under our experimental conditions. This supports an earlier claim of (3+2) REMPI made by Strohaber *et al.*.[27]

A similar analysis of parent ionization dynamics in nitrobenzene is not possible with our data. At all recorded intensities, the nitrobenzene parent ion yield is much smaller than the yields of its fragments; the slope of the parent curve is then heavily influenced by dissociative processes rather than ionization dynamics, and regions of integer slope—if present—would not necessarily be indicative of MPI.

4.2 Dissociative rearrangement

In our aniline spectra, we observe a peak at $m/q = 78$ for which a few different ions could be responsible. We neglect the contributions of the "heavy" ionic phenyl (with a carbon-13) due to relative abundances; one expects $\approx 6.6\%$ of the phenyl ion yield for its heavy partner. This is not consistent with our measurements, which finds these two yields to be nearly identical. A second possible contributor is $C_5H_4N^+$, or any of its isomers. This ion's contribution cannot explicitly be deemed negligible; however, the lack of a complete series of $C_5H_nN^+$ ions makes this assignment dubious.

The remaining contributors are isomers of ionic benzene ($C_6H_6^+$), which must account for the remainder of the $m/q = 78$ peak. While it cannot be determined if benzene was among the impurities in the 99.5%-purity aniline sample, even an extreme case of sample contamination could not account for an appreciable portion of the $m/q = 78$ peak. Most of these ions must then be formed as aniline interacts with our ionizing radiation, though because of the potential benzene contamination and presence of $C_5H_4N^+$, we refrain from making quantitative statements about the yields. If the amino group splits off from the phenyl ring following intense-field excitation, a molecular rearrangement may occur, leaving an amino-originating hydrogen atom with the ring to form ionic benzene and a neutral NH radical:

$$PhNH_2^* \longrightarrow Ph^+ + {}^\bullet NH_2 + e^- \longrightarrow PhH^+ + {}^\bullet NH + e^-$$

Note that this reaction is meant to be illustrative rather than prescriptive. The relatively weak NH_2^+ yield in Fig. 4 additionally lends itself to the notion that, at least in the ionic state, the intact side-group is not a preferred final state of the system.

By the same logic, we can identify a strikingly similar rearrangement process in nitrobenzene. We observe PhO^+ ($m/q = 93$) in our nitrobenzene spectra, which under single-molecule conditions would require an oxygen atom leaving the nitro group to join the phenyl ring, as below:

$$PhNO_2^* \longrightarrow Ph^+ + {}^\bullet NO_2 + e^- \longrightarrow PhO^+ + {}^\bullet NO + e^-$$

This particular rearrangement in nitrobenzene is not a novel observation, as this process has been previously documented under different experimental conditions.[28–30]

5 Conclusion

The ultrafast photoionization and photofragmentation of aniline and nitrobenzene have been comparatively investigated using 800-nm, 50-fs laser pulses with intensities between 6×10^{12} W/cm^2 and 3×10^{14} W/cm^2, without the focal volume effect. Our investigation confirms that, though the two molecules are structural analogues, the opposing electronic behavior of their respective functional groups[17,18] is responsible for some strikingly different photodynamical behavior under intense-field conditions. In the aniline ion mass spectra, the dominance of the singly-charged parent ion, presence of multiply-charged parent ions, and suppression of most dissociative fragmentation processes suggest that the electron-donating nature of the amino group stabilizes the molecule. In the nitrobenzene ion mass spectra, the suppression of the singly-charged parent ion, absence of multiply-charged parent ions, and dominance of ionic fragments suggest that the electron-withdrawing nature of the nitro group does the opposite. While the donating and withdrawing character of the side-groups has long been known to affect the molecules' reactive properties, we demonstrate that the substituent effect is similar regard to stability against intense-field fragmentation. Studies of other amino- and nitro-substituted organic molecules such as *p*-phenylenediamine ($C_6H_4(NH_2)_2$), *p*-dinitrobenzene ($C_6H_4(NO_2)_2$), and *p*-nitroaniline ($C_6H_4NH_2NO_2$) may shed more light on the nature of these effects.

6 Acknowledgments

The authors acknowledge the Max Planck Institute of Quantum Optics in Germany, specifically Dr. Hartmut Schröder, for lending us the reflectron used in these experiments. This material is based upon work supported by the National Science Foundation Grant Nos. PHY-0855675 and PHY-1005071, as well as the National Science Foundation EPSCoR RII Track-2 CA Award No. IIA-1430519

(Cooperative Nebraska-Kansas grant).

References

1 S. Baker, J. S. Robinson, C. A. Haworth, H. Teng, R. A. Smith, C. C. Chirila, M. Lein, J. W. Tisch and J. P. Marangos, *Science*, 2006, **312**, 424–427.

2 C. I. Blaga, J. Xu, A. D. DiChiara, E. Sistrunk, K. Zhang, P. Agostini, T. A. Miller, L. F. DiMauro and C. D. Lin, *Nature*, 2012, **483**, 194–197.

3 J. Yang, X. Zhu, T. J. A. Wolf, Z. Li, J. P. F. Nunes, R. Coffee, J. P. Cryan, M. Gühr, K. Hegazy, T. F. Heinz, K. Jobe, R. Li, X. Shen, T. Veccione, S. Weathersby, K. J. Wilkin, C. Yoneda, Q. Zheng, T. J. Martinez, M. Centurion and X. Wang, *Science*, 2018, **361**, 64–67.

4 J. P. Marangos, *J. Phys. B*, 2016, **49**, 132001.

5 F. Calegari, A. Trabattoni, A. Palacios, D. Ayuso, M. C. Castrovilli, J. B. Greenwood, P. Decleva, F. Martín and M. Nisoli, *J. Phys. B*, 2016, **49**, 142001.

6 M. C. E. Galbraith, C. T. L. Smeenk, G. Reitsma, A. Marciniak, V. Despré, J. Mikosch, N. Zhavoronkov, M. J. J. Vrakking, O. Kornilov and F. Lépine, *Phys. Chem. Chem. Phys.*, 2017, **19**, 19822–19828.

7 A. Perveaux, D. Lauvergnat, F. Gatti, G. J. Halász, A. Vibók and B. Lasorne, *J. Phys. Chem. A*, 2014, **118**, 8773–8778.

8 A. I. Kuleff and L. S. Cederbaum, *J. Phys. B*, 2014, **47**, 124002.

9 M. Nisoli, P. Decleva, F. Calegari, A. Palacios and F. Martín, *Chem. Rev.*, 2017, **117**, 10760–10825.

10 V. Despré, A. Marciniak, V. Loriot, M. C. E. Galbraith, A. Rouzée, M. J. J. Vrakking, F. Lépine and A. I. Kuleff, *J. Phys. Chem. Lett.*, 2015, **6**, 426–431.

11 M. C. E. Galbraith, S. Scheit, G. Golubev, G. Reitsma, N. Zhavoronkov, V. Despré, F. Lépine, A. I. Kuleff, M. J. J. Vrakking, O. Kornilov, H. Köppel and J. Mikosch, *Nature Comm.*, 2017, **8**, 1–7.

12 C. Arnold, O. Vendrell, R. Welsch and R. Santra, *Phys. Rev. Lett.*, 2018, **120**, 123001.

13 T. D. Scarborough, D. B. Foote and C. J. G. J. Uiterwaal, *J. Chem. Phys.*, 2012, **136**, 054309.

14 T. D. Scarborough, J. Strohaber, D. B. Foote, C. J. McAcy and C. J. G. J. Uiterwaal, *Phys. Chem. Chem. Phys.*, 2011, **13**, 13783–13790.

15 J. McMurry, *Organic Chemistry 7th edition*, Brooks/Cole, 2007.

16 S. G. Lias, *NIST Chemistry WebBook, NIST Standard Reference Database Number 69*, National Institute of Standards and Technology, Gaithersburg MD, 20899.

17 H. Zhang, X. Jiang, W. Wu and Y. Mo, *Phys. Chem. Chem. Phys.*, 2016, **18**, 11821.

18 O. A. Stasyuk, H. Szatylowicz, T. M. Krygowski and C. Fonseca Guerra, *Phys. Chem. Chem. Phys.*, 2016, **18**, 11624.

19 A. E. Siegman, *Lasers*, University Science Books, Sausalito, CA, 1986.

20 J. Strohaber and C. J. G. J. Uiterwaal, *Phys. Rev. Lett.*, 2008, **100**, 023002.

21 D. B. Foote, T. D. Scarborough and C. J. G. J. Uiterwaal, *J. Am. Soc. Mass Spectrom.*, 2012, **23**, 834.

22 Z. Deng and J. H. Eberly, *J. Opt. Soc. Am. B*, 1985, **2**, 486–493.

23 F. H. M. Faisal, *Lectures on Ultrafast Intense Laser Science 1*, Springer-Verlag Berlin Heidelberg, 2010, pp. 1–40.

24 J. O. F. Thompson, R. A. Livingstone and D. Townsend, *J. Chem. Phys.*, 2013, **139**, 034316.

25 Y. Honda, M. Hada, M. Ehara and H. Nakatsuji, *J. Chem. Phys.*, 2002, **117**, 2045.

26 T. Ebata, C. Minejima and N. Mikami, *J. Phys. Chem. A*, 2002, **106**, 11070–11074.

27 J. Strohaber, T. Mohamed, N. Hart, F. Zhu, R. Nava, F. Pham, A. A. Kolomenskii, H. Schroeder, G. G. Paulus and H. A. Schuessler, *Phys. Rev. A*, 2011, **84**, 063414.

28 A. D. Tasker, L. Robson, K. W. D. Ledingham, T. McCanny, S. M. Hankin, P. McKenna, C. Kosmidis, D. A. Jaroszynski and D. R. Jones, *J. Phys. Chem. A*, 2002, **106**, 4005–4013.

29 M.-F. Lin, Y. T. Lee and C.-K. Ni, *J. Chem. Phys.*, 2007, **126**, 064310.

30 D. B. Galloway, J. A. Bartz, L. G. Huey and F. F. Crim, *J. Chem. Phys.*, 1993, **98**, 2107.

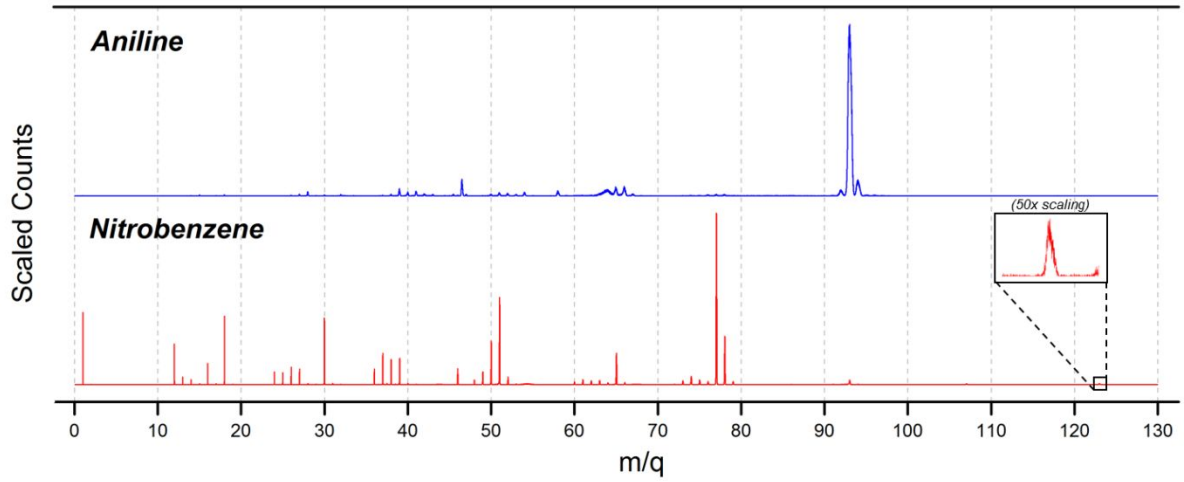

Intense-field stability of photoionization and fragmentation are compared for aniline (C_6H_5-NH_2) and nitrobenzene (C_6H_5-NO_2), with amine vs. nitro substitutions explored.